ELSEVIER

Wave Motion 20 (1994) 151–163

WAVE MOTION

# Eigenmodes of the time reversal operator: A solution to selective focusing in multiple-target media

Claire Prada and Mathias Fink

*Laboratoire Ondes et Acoustique, URA CNRS 1503, Université Paris VII, ESPCI, 10 rue Vauquelin, 75005, Paris, France*

Received 4 April 1994

**Abstract**

The iterative time reversal mirror provides an elegant way of focusing in multiple target media on the most reflective one. This paper presents a method to focus on the other targets. It is derived from a theoretical study of the iterative time reversal process. The iterative process can be described at each frequency by a time reversal operator which can be diagonalized. The eigenvectors of this operator are eigenmodes of the time reversal process. In the case of well resolved targets of different "brightness", the rank of the time reversal operator is equal to the number of targets and each eigenvector of non zero eigenvalue provides the optimal phase and amplitude law to focus on the corresponding target. An experimental validation of these results is given.

## 1. Introduction

The invariance under time reversal of some physical systems is a very fascinating and attractive property. Who has never dreamt of going backward in time? But this invariance is very difficult to put in evidence experimentally. The large number of parameters involved in most systems explains why irreversibility is generally observed.

In the domain of acoustic waves, the small number of degrees of freedom allows to achieve a time reversal operation. An acoustic wave can be time reversed by means of a time reversal mirror [1–9]. Such a mirror is made of a large array of piezoelectric transducers that is able to measure and to produce an instantaneous pressure field. Each transducers is connected to its own electronical device consisting of a receiving amplifier, an A/D converter, a storage memory and a programmable transmitter. All these channels are parallel processed for reception as well as for transmission.

This ability to time reverse an ultrasonic wave has significant consequences on techniques of ultrasonic focusing which is a general problem in acoustic. This problem arises in many applications such as non-destructive testing, medical techniques (lithotripsy and hyperthermia) or underwater acoustics.

In classical methods, the focusing of an acoustic wave with an array of transducers requires a knowledge of the geometry of the array, the sound speed in the medium and the position of the target. Then, the delay for each transducer can be computed in order to focus on the target. But with large arrays of transducers, strong geometrical distortions may occur leading to significant errors. Furthermore, if the propagating medium is not homogeneous, the time delay can not easily be computed.

For a reflective target adaptive time delay focusing technique can be used [10]. A first wide wave is transmitted to the medium in order to get an echo from the target. The delays are estimated by a cross correlation

0165-2125/94/$07.00 
*SSDI* 0165-2125(94)00020-6

technique. Unfortunately, these methods require a pointlike scatterer. They are not efficient if there are several targets. Furthermore they assume that the propagating medium only induces time delay distortion in the wavefront. In many cases, a wave propagating in an inhomogeneous medium is not only delayed but its spatial and temporal shape is also distorted through refraction, diffraction and multiple scattering. These distortions are not taken into account by time delay focusing.

The time reversal operation is an elegant way of avoiding all these problems. The geometrical errors as well as the sound speed fluctuations are compensated automatically by this self-adaptive process. Furthermore, if there are several targets, the time reversal process can be iterated in order to focus one the most reflective ones.

As shown in several papers [2–7], the acoustic iterative time reversal mirror is a very efficient system to focus automatically among a set of well resolved targets, on the most reflective one. A question arises: is there a way to focus on the other targets? This would be useful for instance in lithotripsy when several lithiases exist. It may also be interesting for target classification. An answer to this question was found in the theory of the iterative time reversal process. This theory was built in order to get a better understanding of the convergence of the iterative time reversal process. It is based on a matrix formalism: the array of $N$ transducers in a given medium is considered as a linear and time invariant system of $N$ inputs/$N$ outputs. It relies on the definition of the transfer matrix $K$ of the system and of the time reversal operator $K^*K$.

The results shown in the following are general. They only assume that the propagation of waves is linear and that an array of transmit-receive elements is used. Furthermore they might be applied to other linear waves.

The first part of the paper is a brief summary of the principle of acoustic time reversal mirrors. The second part provides the theory of the iterative time reversal process with the definition of the time reversal operator. The third part deals with the particular case of pointlike scatterers. The fourth part shows how a detection and focusing method is deduced from the preceeding theory and it provides experimental examples.

## 2. The iterative time reversal mirror

### 2.1. Time reversal of an ultrasonic wave

In the linear regime, in a fluid medium, an ultrasonic pressure wave $P(\boldsymbol{r}, t)$ satisfies the equation

$$\kappa(\boldsymbol{r}) \frac{\partial^2 P}{\partial t^2} = \nabla\left(\frac{\nabla P}{\rho(\boldsymbol{r})}\right), \tag{1}$$

where $\kappa(\boldsymbol{r})$ is the compressibility and $\rho(\boldsymbol{r})$ is the density of the medium.

This equation contains only a second derivative with respect to the temporal variable which provides the strong property of being invariant under time reversal. In other words, if the pressure wave $P(\boldsymbol{r}, t)$ satisfies the Eq. (1) then the time reversed wave $P(\boldsymbol{r}, -t)$ also satisfies Eq. (1). In particular, if $P(\boldsymbol{r}, t)$ is a wave issued from a source then $P(\boldsymbol{r}, -t)$ is a wave focusing on the source. The problem is how to produce the time reversed version of a given wave. In the case of an ultrasonic wave this can be achieved with large arrays of transducers.

### 2.2. The time reversal mirror

A time reversal mirror is an array of transducers, each connected to its own memory and to its own programmable generator. It is used in an inhomogenous medium to convert a wave emerging from a source whose position is unknown, into a wave converging on the source. Usually, the source is an insonified scatterer. The time reversal process operates as follows (Fig. 1):

(1) A wide incident wave is transmitted by the array of transducers.
(2) The wave reflected by the target is detected by the array, the echographic signals are recorded in the memories.
(3) The signals are time reversed and used to transmit a wave converging to the target in spite of the sound speed fluctuations in the medium.

The efficiency of such a process to focus through an inhomogeneous medium has been demonstrated in Refs. [2–10].

### 2.3. The iterative time reversal process

#### 2.3.1. Principle

In the case of several targets, one time reversal process does not lead to a one-point focussed wave, but the process can be iterated in order to focus on the most

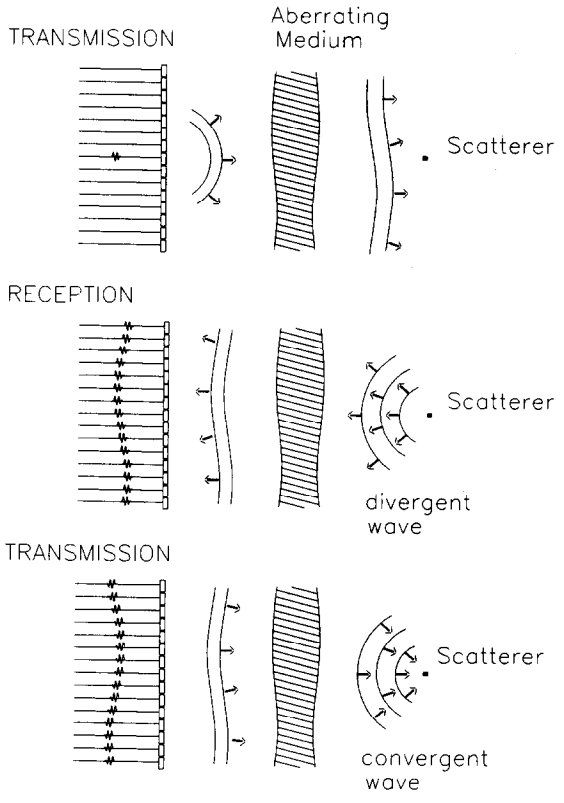


Fig. 1. Self-focusing through an inhomogeneous medium with a time reversal mirror.

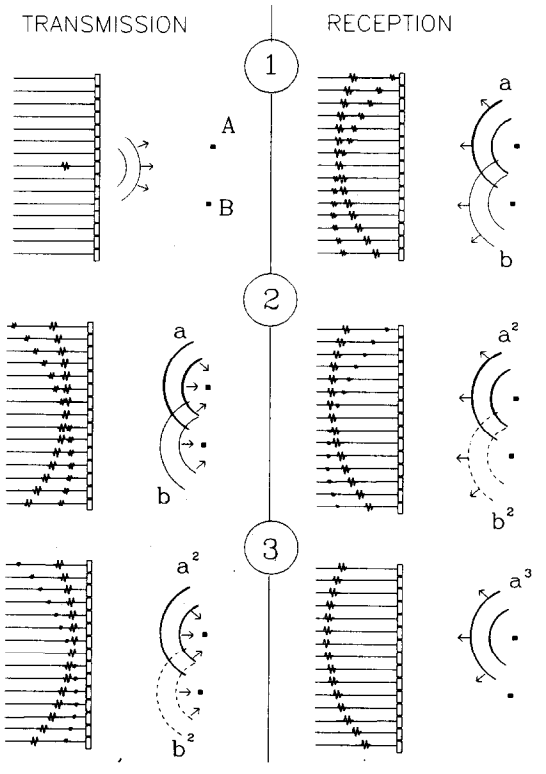


Fig. 2. Iteration of the time reversal process.

reflective target. Indeed, the wave transmitted after one time reversal process leads to a second reflected wave that can also be measured and time reversed. For instance, we consider two targets A and B of reflectivities $a$ and $b$ $(a>b)$, we assume that they are well resolved by the array of transducers and placed at the same distance from the array (Fig. 2), and that only singly scattering is significant. Then the first time reversed wave is the sum of a wave focussed on A of relative amplitude $a$ and a wave focussed on B of relative amplitude $b$. Those two waves are reflected by the targets which produces two spherical waves of amplitudes $a^2$ and $b^2$. After $n$ iterations of the process, the relative amplitudes are $a^n$ and $b^n$, so that if $n$ is big enough the wave focusing on B is negligible, and the system learns automatically how to focus on target A.

### 2.3.2. *Experiment*

To demonstrate the ability of the iterative mode of TRM to select the most reflective target, a linear array of 64 rectangular transducers is used. The array elements are 0.6 mm wide and spaced 0.75 mm. The target is made of two wires of different reflectivities placed perpendicular to the array at a depth of 90 mm.

The first wave is transmitted by one element in the center of the array. It is wide in order to insonify both wires. The two wavefronts corresponding to each target can easily be observed (Fig. 3a). The time reversal process is iterated. The signals received on the array after iteration 1, 2 and 3 are displayed on Figs. 3b, 3c and 3d. On Fig. 3d, only the wavefront corresponding to the most reflective wire remains, this wire has been selected automatically. In order to confirm this selection, the field produced at each iteration was measured by a needle hydrophone. At the first time reversal operation, the pressure diagram presents two lobes at the position of the wires, one is higher than the other. At the second and the third iterations the level of the lower peak decreases. At the fourth, the wave focuses on the most reflective target (Fig. 4).

This experimental example is quite simple and in general the targets can be at different distances from the array or not so well resolved, and they can have the same reflectivities. Furthermore, there might be more

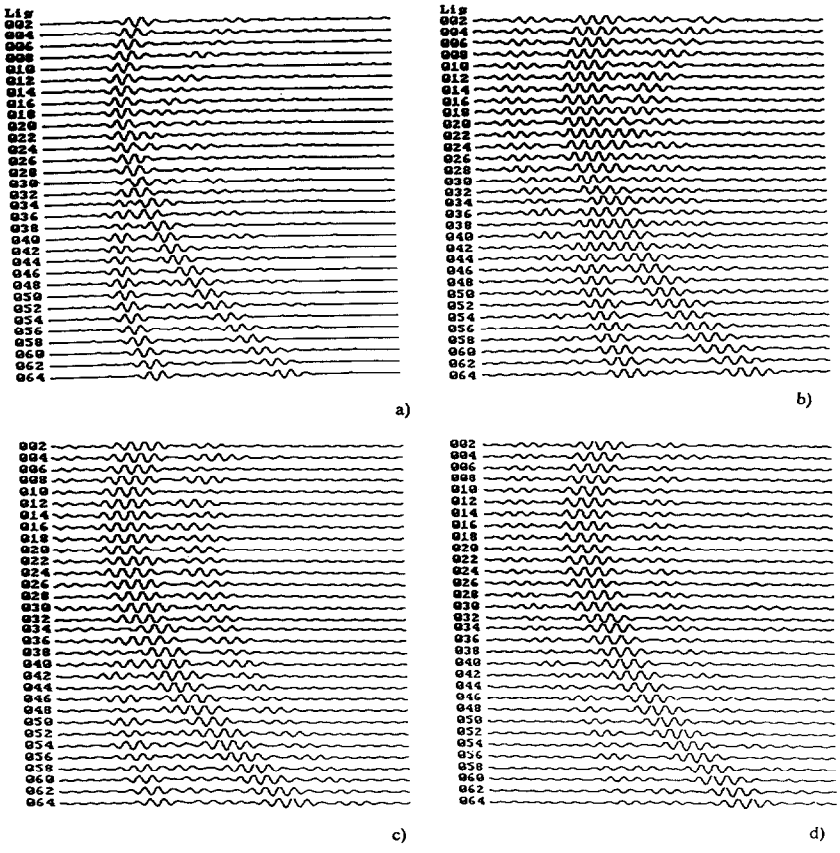


Fig. 3. First experiment: Echos of the two wires received by the transducers for iterations 1 to 4. The figure shows every other signal.

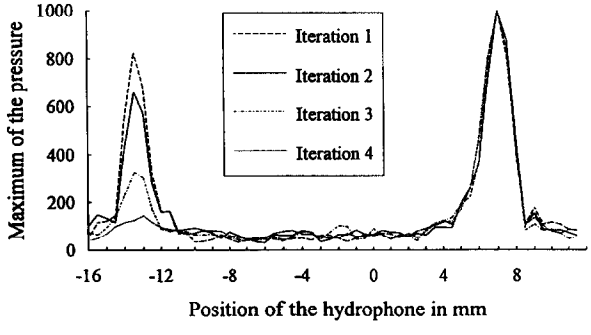


Fig. 4. First experiment: Maximum of the pressure measured in the plane of the two wires after iterations 1 to 4.

than two targets. In order to understand how the different parameter of the number of targets, their reflectivities and their sizes influence the time reversal process, a theory has been developed. It relies on the difinition of the transfer matrix of the system and on the time reversal operator in the harmonic regime.

## 3. The time reversal operator

The principle of the iterative time reversal process has been presented. In order to describe theoretically such a process, we give a simple formulation of any transmit and receive operation made with an array of reversible transducers. The idea is to express in a general manner the received signals as a function of the transmitted ones. An array of $L$ transmit-receive transducers insonifiing a scattering medium is considered. The whole system is supposed to be time-invariant and linear. In other words, it is assumed that the behavior of the transducers is linear and the waves obey the laws of linear acoustics.

### *3.1. Inter element impulse response*

In order to express the received signals as functions of the transmitted ones, we define for each pair of trans-

ducers, an inter element impulse response. This response includes all the propagation effects through the medium under investigation as well as the acousto-electric responses of the two elements. The inter element impulse response $k_{lm}(t)$ from the element $m$ to the element $l$ is the signal received on the channel number $l$ after a temporal Delta function is applied to the channel number $m$ (Fig. 5). As the transformations are supposed to be linear and time-invariant, the $L^2$ temporal functions $k_{lm}(t)$ for $1 \leqslant l \leqslant L$ and $1 \leqslant m \leqslant L$ can describe any transmit-received operation for the same arrangement. Indeed, let $e_m(t)$, $1 \leqslant m \leqslant L$, be the $L$ input signals, then the output signals $r_l(t)$, $1 \leqslant l \leqslant L$, are given by

$$r_l(t) = \sum_{m=1}^{L} k_{lm}(t) \otimes_t e_m(t), \quad 1 \leqslant l \leqslant L. \tag{2}$$

### 3.2. Multiple input/multiple output formalism: the transfer matrix

A temporal Fourier transform leads to the following relation

$$R_l(\omega) = \sum_{m=1}^{L} K_{lm}(\omega) E_m(\omega), \quad 1 \leqslant l \leqslant L. \tag{3}$$

Eq. (3) is simplified using a matrix formula:

$$\boldsymbol{R}(\omega) = \mathbf{K}(\omega)\boldsymbol{E}(\omega) \tag{4}$$

where $\boldsymbol{E}(\omega) = (E_l(\omega))_{1 \leqslant l \leqslant L}$ is the column vector of the Fourier transform of the transmit signals, and $\boldsymbol{R}(\omega) = (R_l(\omega))_{1 \leqslant l \leqslant L}$ is the column vector of the Fourier transform of the received signals. In the following, those two vectors will be called the input and the output signals. Also, $\mathbf{K}(\omega) = (K_{lm}(\omega))_{1 \leqslant m,l \leqslant L}$ is called the transfer matrix. Note that the model is very general in the sense that no assumption is made on the responses $k_{lm}(t)$. Complex phenomena such as mechanical or electronical cross couplings between transducer elements may be taken into account provided they are linear.

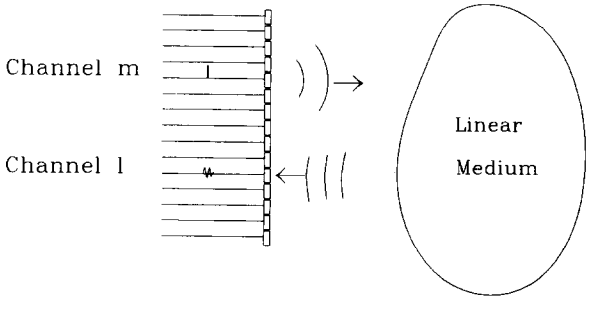


Fig. 5. Inter element impulse responses.

### 3.3. Reciprocity theorem and symmetry of the transfer matrix

The reciprocity theorem is well known for propagation in inhomogeneous media [11]. It indicates that the position of a point source and an observer can be reversed without altering the acoustic field. A consequence of that theorem is that the inter element impulse response from element number $m$ to element number $l$ is equal to the inter element impulse response from element number $l$ to element number $m$, so that $K_{lm}$ is equal to $K_{ml}$. In other words the matrix $\mathbf{K}$ is symmetrical. This property is very important in the following. In the fourth section we provide a theoretical demonstration for pointlike scatterers and an array of similar transducers (see Eq. (17)).

### 3.4. The iterative time reversal process

The iterative time reversal process can now be described: This paragraph provides a mathematical formulation of the iterative process. The operator linking the input signals from one iteration to another is given. This description is made at one given frequency, so we omit the term $\omega$ in the following.

The matrix relation between transmitted and received signals allows us to establish an expression of the emitted signal for any number of iterations. Let $\boldsymbol{E}^0$ be the initial input vector signal. The output is then $\boldsymbol{R}^0 = \mathbf{K}\boldsymbol{E}^0$.

The time reversal operation is equivalent to a phase conjugation in the frequency domain, so that the new input signal $\boldsymbol{E}^1$ is the phase conjugate of the preceeding output signal $\boldsymbol{R}^0$

$$\boldsymbol{E}^1 = \mathbf{K}^* \boldsymbol{E}^{0*}.$$

The new output signal is then

$$\boldsymbol{R}^1 = \mathbf{K}\boldsymbol{E}^1.$$

In the same way, the input signals at the second and third iterations are

$$\boldsymbol{E}^2 = \mathbf{K}^* \boldsymbol{E}^{1*} = \mathbf{K}^* \mathbf{K} \boldsymbol{E}^0,$$

These formulas can easily be generalized by induction: the input signal at the iterations number $2n$ and $2n+1$ are given by

$$\boldsymbol{E}^{2n} = [\mathbf{K}^*\mathbf{K}]^n \boldsymbol{E}^0 ,$$

$$\boldsymbol{E}^{2n+1} = [\mathbf{K}^*\mathbf{K}]^n \mathbf{K}^* \boldsymbol{E}^{0*} . \qquad (5)$$

The issue of the iterative process depends on the asymptotic behavior of the operator $[\mathbf{K}^*\mathbf{K}]^n$.

### 3.5. Behavior of $[\mathbf{K}^*\mathbf{K}]^n$: convergence of the process

The behavior of $[\mathbf{K}^*\mathbf{K}]^n$ can be determined because the matrix $\mathbf{K}^*\mathbf{K}$ can be diagonalized. The symmetry of $\mathbf{K}$ implies that the operator $\mathbf{K}^*\mathbf{K}$ is hermitian. Indeed, we have

$${}^t[\mathbf{K}^*\mathbf{K}]^* = {}^t[\mathbf{K}\mathbf{K}^*] = {}^t\mathbf{K}^* {}^t\mathbf{K} = \mathbf{K}^*\mathbf{K} ,$$

where ${}^t\mathbf{K}$ means the transpose matrix of $\mathbf{K}$. According to the theory of hermitian operators, $\mathbf{K}^*\mathbf{K}$ can be diagonalized, its eigenvectors are orthogonal and its eigenvalues are real. Furthermore, the eigenvalues are positive [1].

The operator $\mathbf{K}^*\mathbf{K}$ has $p$ ($p \leqslant L$) distinct eigenvalues $\lambda_1 < \lambda_2 < \cdots < \lambda_p$. Let $F_1, F_2, \ldots, F_p$ be the eigenspaces associated to these eigenvalues. Any vector can be written as the sum of vectors of the eigenspaces. We assume that the decomposition of the first transmitted signal $\boldsymbol{E}^0$ in terms of the eigenspace $F_i$ is given by

$$\boldsymbol{E}^0 = \boldsymbol{V}_1 + \boldsymbol{V}_2 + \cdots + \boldsymbol{V}_p$$

$$\text{with } \boldsymbol{V}_1 \neq 0 \text{ and } \boldsymbol{V}_i \in F_i , \qquad (6)$$

where $\boldsymbol{V}_1, \boldsymbol{V}_2, \ldots, \boldsymbol{V}_p$ are different eigenmodes of the iterative time reversal process. Then the input signal after $2n$ time reversal operations is

$$\boldsymbol{E}^{2n} = [\mathbf{K}^*\mathbf{K}]^n \boldsymbol{E}^0 = \lambda_1^n \boldsymbol{V}_1 + \lambda_2^n \boldsymbol{V}_2 + \cdots + \lambda_p^n \boldsymbol{V}_p ,$$

so that

$$\boldsymbol{E}^{2n} \approx \lambda_1^n \boldsymbol{V}_1 \quad \text{for large values of } n . \qquad (7)$$

For an odd number of iterations, the decomposition of $\mathbf{K}^*\boldsymbol{E}^{0*}$ over the eigenspace is required, Eq. (6) leads to

$$\mathbf{K}^*\boldsymbol{E}^{0*} = \mathbf{K}^*\boldsymbol{V}_1^* + \mathbf{K}^*\boldsymbol{V}_2^* + \cdots + \mathbf{K}^*\boldsymbol{V}_p^* . \qquad (8)$$

It is easily proven that $\mathbf{K}^*\boldsymbol{V}_i^*$ is an eigenvector with the eigenvalue $\lambda_i$ [2]. Then the input signal at the iteration number $2n+1$ is

$$\boldsymbol{E}^{2n+1} = [\mathbf{K}^*\mathbf{K}]^n \mathbf{K}^*\boldsymbol{E}^{0*} = \lambda_1^n \mathbf{K}^*\boldsymbol{V}_1^* + \lambda_2^n \mathbf{K}^*\boldsymbol{V}_2^* + \cdots + \lambda_p^n \mathbf{K}^*\boldsymbol{V}_p^*$$

so that

$$\boldsymbol{E}^{2n+1} \approx \lambda_1^n \mathbf{K}^*\boldsymbol{V}_1^* \text{ for large values of } n. \qquad (9)$$

Generally, $\lambda_1$ is nondegenerate and the limits are shown to be [3]

$$\boldsymbol{E}^{2n+1} \approx \lambda_1^{n+1/2} e^{j\Phi} \boldsymbol{V}_1 \text{ for large values of } n . \qquad (10)$$

This result insures the convergence of the iterative process towards odd and even limits. In general, the two limits differ by a phase factor.

This analysis shows that the iterative time reversal process has eigenmodes that are the eigenvectors of the time reversal operator. A physical interpretation of the eigenmodes is given in Section 4, for the case of well resolved pointlike scatterers.

## 4. Determination of the transfer matrix: pointlike targets and single scattering

### 4.1. The transfer matrix

If there are $D$ pointlike scatteres, the transfer matrix can be written as the product of three matrices (Fig. 6):

(1) a propagation matrix that describes the transmission and the propagation from the transducers to the targets,

(2) a scattering matrix which is diagonal for the case of single scattering.

(3) the back propagation matrix which is the transpose of the propagation matrix because of the reciprocity principle.

We assume that the array of transducers is made of $L$ similar elements and that the medium contains $d$ pointlike scatterers with reflectivity coefficients

[1] Let $\lambda$ be an eigenvalue of $\mathbf{K}^*\mathbf{K}$ and $\boldsymbol{V}$ an associated eigenvector. We have $\mathbf{K}^*\mathbf{K}\boldsymbol{V} = \lambda\boldsymbol{V}$ so that ${}^t\boldsymbol{V}^*\ \mathbf{K}^*\mathbf{K}\boldsymbol{V} = {}^t\boldsymbol{V}^*\lambda\boldsymbol{V} = \lambda\|\boldsymbol{V}\|^2$. Because $\mathbf{K}$ is symmetrical we have $\|\mathbf{K}\boldsymbol{V}\|^2 = {}^t(\mathbf{K}\boldsymbol{V})^*(\mathbf{K}\boldsymbol{V}) = {}^t\boldsymbol{V}^*\mathbf{K}^*\mathbf{K}\boldsymbol{V}$. It follows that $\|\mathbf{K}\boldsymbol{V}\|^2 = \lambda\|\boldsymbol{V}\|^2$ and $\lambda$ is positive.

[2] Indeed, $[\mathbf{K}^*\mathbf{K}]\mathbf{K}^*\boldsymbol{V}_i^* = \mathbf{K}^*[\mathbf{K}^*\mathbf{K}\boldsymbol{V}_i]^* = \lambda_i \mathbf{K}^*\boldsymbol{V}_i^*$.

[3] Indeed, $\|\mathbf{K}^*\boldsymbol{V}_1^*\|^2 = \boldsymbol{V}_1^*\mathbf{K}^*\mathbf{K}\boldsymbol{V}_1 = \lambda_1\|\boldsymbol{V}_1\|^2$.

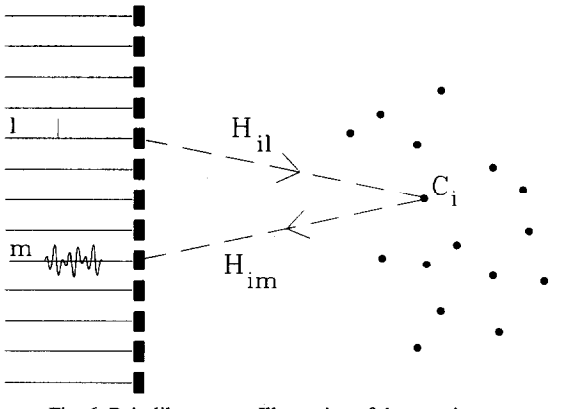


Fig. 6. Pointlike targets: Illustration of the notations.

$C_1, C_2, \ldots, C_d$. For instance, in the case of Rayleigh scatterers the $C_i$ are proportional to the square of the frequency.

Let $h_{il}(t)$ be the diffraction impulse response [12] of the transducer number $l$ to the scatterer number $i$. Let $a_e(t)$ and $a_r(t)$ be the transducers acousto-electrical response in emission and in reception, with Fourier transforms $A_e(\omega)$ and $A_r(\omega)$.

*4.1.1. Propagation*

If the input signal at each element $l$ is $e_l(t)$, then the pressure at the scatterer $i$ is

$$p_i(t) = \sum_{l=1}^{L} e_l(t) \otimes_t a_e(t) \otimes_t h_{il}(t) \,. \tag{11}$$

This is written in the frequency domain as

$$P_i = A_a \sum_{l=1}^{L} E_l H_{il} \,. \tag{12}$$

This expression is simplified using a matrix notation:

$$\boldsymbol{P} = A_e \mathbf{H} \boldsymbol{E} \,, \tag{13}$$

where $\boldsymbol{E}$ is the input signal as in part II, $\boldsymbol{P}$ is the vector of the pressure received by the $d$ scatterers and $\mathbf{H}$ is a matrix of dimension $L \times d$ called the diffraction matrix.

$$\mathbf{H} = \begin{pmatrix} H_{11} & H_{12} & \ldots & H_{1L} \\ H_{21} & H_{22} & \ldots & H_{2L} \\ \vdots & \vdots & \ddots & \vdots \\ H_{d1} & H_{d2} & \ldots & H_{dL} \end{pmatrix} = (H_{il})_{(1 \leqslant i \leqslant d, 1 \leqslant l \leqslant L)} \tag{14}$$

*4.1.2. Single scattering*

In the case of single scattering, the pressure reflected by the scatterer number $i$ and noted $Q_i$ depends only on the pressure $P_i$ received by the same scatterer through the linear relation $Q_i = C_i P_i$. Therefore, the vectors $\boldsymbol{P}$ and $\boldsymbol{Q}$ are linked by a diagonal matrix $\mathbf{C}$ as follows

$$\boldsymbol{Q} = \mathbf{C}\boldsymbol{P} \tag{15}$$

where $C_{ij} = \delta_{ij} C_i$ for all $i,j \in 1, \ldots, d$. This matrix can also be expressed quite simply for double scattering.

*4.1.3. Back propagation*

According to the reciprocity principle, the back propagation matrix is the transpose of the propagation matrix $\mathbf{H}$ so that the vector of the pressure reflected by the $d$ scatterers, $\boldsymbol{Q}$, is linked to the output signal $\boldsymbol{R}$ by the relation

$$\boldsymbol{R} = A_r {}^t\mathbf{H}\boldsymbol{Q} \tag{16}$$

Finally, the transfer matrix is given by

$$\mathbf{K} = A_e A_r {}^t\mathbf{H}\mathbf{C}\mathbf{H} \tag{17}$$

It can be seen from Eq. (17) that the transfer matrix is symmetrical.

*4.2. Ideal separation of the targets: determination of the eigenvectors of* $\mathbf{K}^*\mathbf{K}$

The reflectors are said to be ideally separated when it is possible to focus on one of them without sending energy to the others. Suppose that a pointlike source is placed at the position of the reflector number $i$ and emits a temporal signal $\delta(t)$. Then, the signal received on the transducer number $l$ is the convolution of the impulse diffraction response of the element number $l$ to the scatterer number $i$ with the acousto-electrical response in reception $a_r(t)$, that is to say $a_r(t) \otimes_t h_{il}(t)$. The best way to focus on the same reflector, is to use as input signals the time-reversed signals $a_r(-t) \otimes_t h_{il}(-t)$. Therefore, the pressure signal received by a reflector number $j$ is in the frequency domain,

$$P_j = A_r^* A_e \sum_{l=1}^{L} H_{jl} H_{il}^* \,. \tag{18}$$

We note that $\boldsymbol{H}_i$ the vector of components $(H_{i1}, H_{i2}, \ldots, H_{iL})$. The Eq. (18) can be written as

$$P_j = A_r^* A_e {}^t\boldsymbol{H}_j \boldsymbol{H}_i^* \,. \tag{19}$$

If the separation is ideal at frequency $\omega$, $P_j$ is almost zero if $j \neq i$. In other words, the vectors $\boldsymbol{H}_i$ are orthogonal. The eigenvectors of $\mathbf{K}^*\mathbf{K}$ are deduced from this last equation (see the proof in the appendix). They are the $\boldsymbol{H}_i^*$ associated to the eigenvalues

$$\lambda_i = |C_i|^2 \left( \sum_{l=1}^{L} |H_{il}|^2 \right)^2 . \tag{20}$$

Each eigenvector of the time reversal operator is associated to one of the pointlike targets. It is exactly (at one frequency) the vector signal that would be emitted after one time reversal process if only this target was present (Fig. 7). As seen in Eq. (20), the eigenvalue depends on the reflectivity of the target as well as on propagating effects. Indeed, it is clear that the apparent reflectivity of a target depends on its position with respect to the array.

## 5. The detection and the selective focusing method

These theoretical results allow us to answer the question: how to focus on a weaker target? Indeed, the transfer matrix of the system can easily be measured. Then, the diagonalization of the time reversal operator provides the amplitude and phase law to focus on each target separately.

### 5.1. The method

*The first step* is the measurement of the inter element impulse response of the system. As the reception is parallel in our system, this measurement requires $N$ transmit-receive operations for an array of $N$ transducers. The first transducers of the array is excited with a signal $e(t)$. The signals received on the $N$ channels are stored. This operation is repeated for all the transducers of the array with the same transmitted signal $e(t)$. The components of the transfer matrix $\mathbf{K}$ are obtained by a Fourier transform of each signal. This measurement could also be done with any multiplexed system by $N \times N$ transmit-receive operations.

*The second step* is the diagonalization of the time reversal operator at the chosen frequency. For this computation the matrix has to be symmetrical which is not the case in the experiments. Indeed, the reciprocity principle is not very well verified because of noise and also because of the differences between the acousto-electrical responses of the transducers, expecially when they have different shapes. So we need first to make the transfer matrix $\mathbf{K}$ symmetrical by replacing each term $K_{lm}$, $1 \leqslant l, m \leqslant N$ by $\frac{1}{2}(K_{lm} + K_{ml})$. The time reversal operator $\mathbf{K}^*\mathbf{K}$ is then calculated and diagonalized.

Then it is very interesting to look at the eigenvalues distribution. In the case of point-like targets, the number of significant eigenvalues is exactly the number of targets, provided they are resolved by the system. More generally, this number corresponds to the number of bright points in the set of targets.

*The third step* is to backpropagate each eigenvector. This can be done either numerically or experimentally. The numerical backpropagation can be computed for an homogeneous medium and an array of well known geometry and provides separated images of the different targets. The experimental backpropagation requires programmable generators controlled in parallel like for the time reversal mirror. Pulsed signals are built from the monochromatic data given by the eigenvectors (see section 5.3.4). This allows us to focus on one of the targets without knowing the geometry of the array of

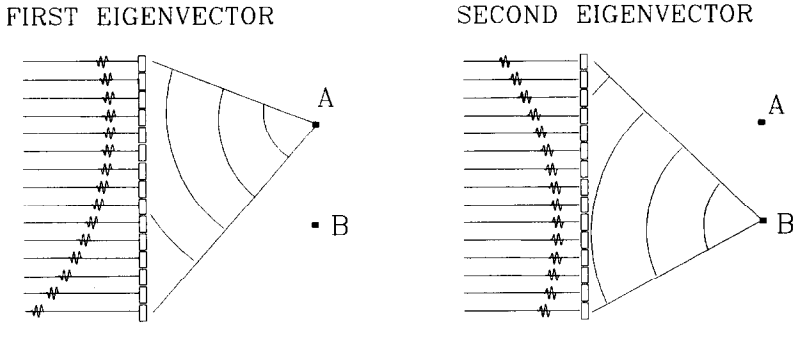


Fig. 7. Illustration of the eigenvectors in the case of two ideally resolved and point-like targets.

transducers nor the properties of the propagating medium.

### 5.2. Second experiment

In this experiment, the iterative time reversal process is compared to the first eigenvector of the operator $K^*K$ at one given frequency.

#### 5.2.1. The experimental set-up

The array of transducers is linear, made of 96 rectangular transducers, spaced by 0.41 mm and operating around the center frequency of 3 MHz. With 96 electronic channels, the received signals are sampled at a frequency of 20 Mhz. The target consists of four wires of different diameters placed perpendicular to the array of transducers at a depth of 90 mm. The first wire is a 0.2 mm diameter copper wire placed at $x_1 = 13$ mm from the array axis, the second is a 0.1 mm diameter copper wire at $x_2 = 8.2$ mm, the third is a 0.2 mm diameter nylon wire placed at $x_3 = 2.9$ mm and the fourth is a 0.4 mm diameter steel wire placed at $x_4 = -4$ mm (Fig. 8).

#### 5.2.2. Iteration of the time reversal process

The time reversal process is iterated four times and at each iteration the reflected signals are stored. As the eigenmodes of the time reversal operator are calculated at one given frequency, the analysis of the iterative process is made at one frequency. The Fourier transform of these signals is computed and the components at 2.7 MHz provides four vector signals one for each iteration. At this frequency the wavelength is 0.56 mm and the resolution cell is 1.2 mm wide, so that the targets are considered as pointlike. The field produced by the propagation of these vectors is calculated and displayed on Fig. 9. At the first iteration, we see the position of the four wires. The lobe corresponding to the steel wire is the higher one. Then comes the 0.2 mm diameter nylon wire, the 0.2 mm diameter copper wire and the 0.1 mm diameter copper wire. The nylon wire is closer to the array axis this is why it gets more energy than the 0.2 mm diameter copper wire. The convergence of the iterative process is rather fast and at the fourth iteration, the steel wire is selected.

#### 5.2.3. Diagonalization of the time reversal operator

After the measurement of the inter element impulse responses, the time reversal operator is computed at frequency 2.7 MHz. The distribution of the eigenvalues shows four significant eigenvalues, the 92 others are almost zero (Fig. 10).

The numerical propagation of the first four eigenvectors provides the position of the four wires. For each eigenvector, a main lobe is observed at the position of one of the wires (Fig. 11). The order of targets corre-

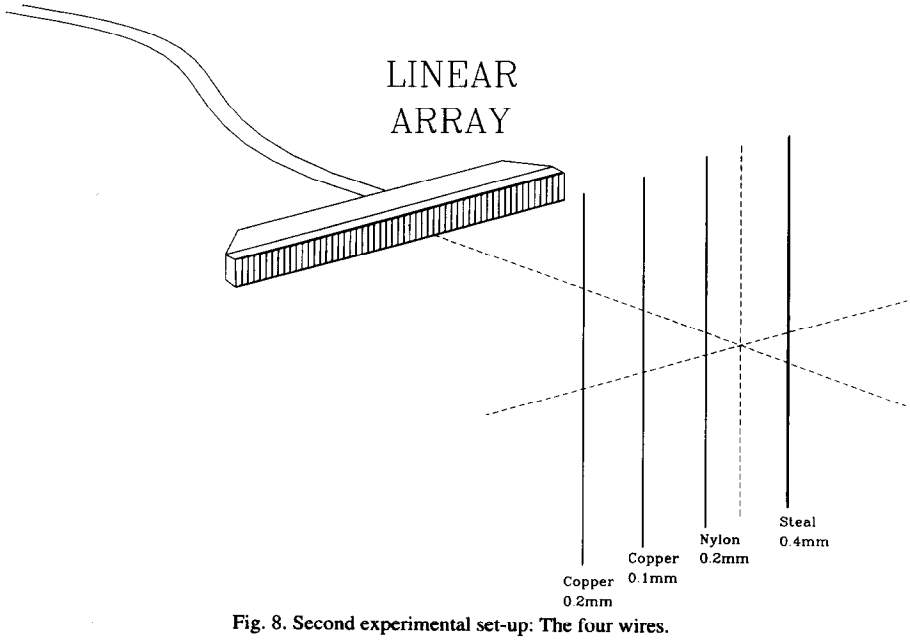


Fig. 8. Second experimental set-up: The four wires.

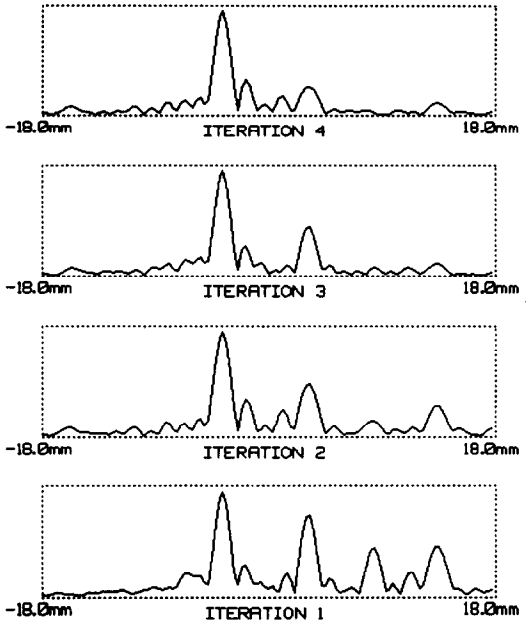


Fig. 9. Second experiment: Field calculated in the plane of the wire at 2.7 MHz for iterations 1 to 4.

sponds exactly to the level of the different lobes observed in Section 5.2.2 after on time reversal process. In particular, the eigenvector associated to the biggest eigenvalue corresponds to the issue of the time reversal process.

### 5.3. Third experiment

This experiment is done with a 2D array and the propagation of the eigenvector is done experimentaly. Furthermore, the targets are not pointlike and quite close to each other.

#### 5.3.1. The experimental set-up

We used a prefocussed sectoralized and annular array of 121 transducers. As 64 electronic channels are available, only 64 elements regularly distributed are used. The focal length of the array is 190 mm and the diameter is 200 mm. The central frequency of the transducers is $f = 360$ kHz. The target is made of two plastic spheres placed in water, a few millimeters from the focus in the focal plane. Their diameters are 7 mm and 5 mm and the distance between their centers is 6 mm. As the wavelength is 4.2 mm and the resolution cell 4 mm large, they are far from ideally resolved pointlike scatterers.

#### 5.3.2. The iterative time reversal process

The time reversal operation has been iterated four times. The first transmitted wave was obtained with the central element of the array. At the fourth iteration of the time reversal process, the pressure field was scanned after replacing the spheres with a needle hydrophone in the focal plane with a 1 mm step (Fig. 13). We observe that the maximum of the pressure is on the center of the biggest sphere but the convergence of the iterative process is slow because of the small distance between the two spheres.

#### 5.3.3. Diagonalization of the time reversal operator

The transmission of the eigenvectors is done experimentally. We choosed to study the time reversal operator at 330 kHz because at this frequency the biggest sphere is selected fast. The distribution of the 64 eigenvalues shows two significant values, meaning that the object has two "bright" points (Fig. 14).

#### 5.3.4. Transmission of the two main eigenvectors

As the eigenvectors are computed at a given frequency, we need to built a pulsed signal from the monochromatic data. The component number $i$ of an eigenvector is a complex quantity of phase $\phi_i$ and amplitude $A_i$. Thus, for transducer number $i$, the pulsed signal is built as a modulated gaussian at frequency $f$ with maximum amplitude $A_i$ and phase shifted by $\phi_i / 2\pi f$. This provides $N$ signals that are then applied to the $N$ transducers. The transmitted field is measured by a

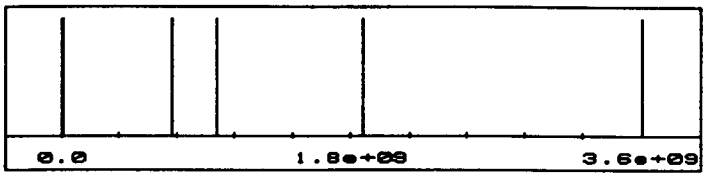


Fig. 10. Second experiment: Distribution of the 96 eigenvalues of the time reversal operator.

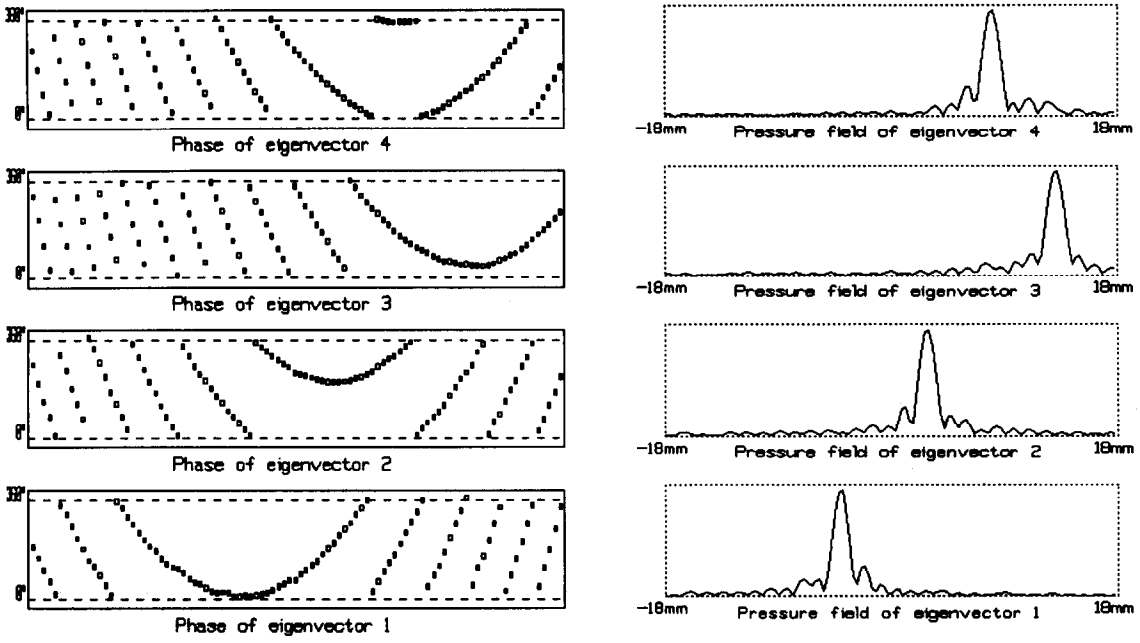


Fig. 11. Second experiment: On the left: phase law of the first four eigenvectors. On the right: field calculated by propagation of the first four eigenvectors.

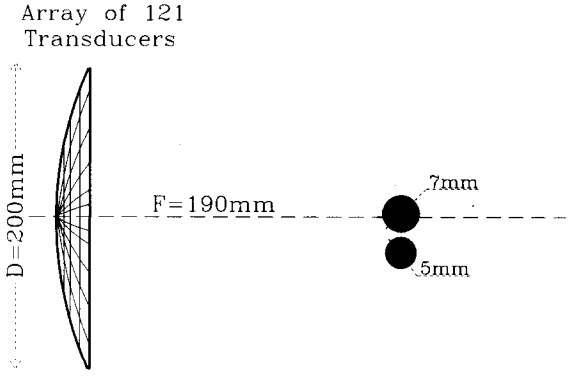


Fig. 12. Third experimental set-up: the two spheres.

needle hydrophone in the focal plane after the targets were removed. This is done for the first and the second eigenvectors. On the pressure diagram, the maximum is observed at the position of the biggest sphere after transmission of the first eigenvector (Fig. 15) and at the position of the second sphere after transmission of the second eigenvector (Fig. 16). This example proves that the transfer matrix method can be applied to targets that are not pointlike nor perfectly resolved.

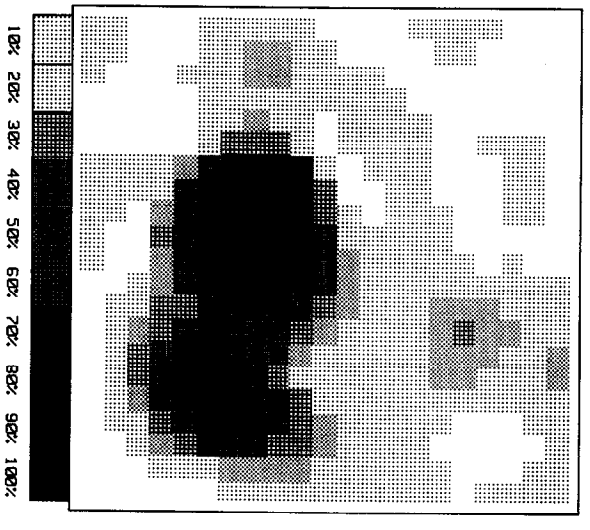


Fig. 13. Third experiment: Scanning of the field produced after four iterations of the time reversal process, scanned area 20×20 mm.

## 6. Conclusion

The goal of this paper was to present a new method of detection and selective focusing in multiple target media. The method is based on the time reversal concept. We introduced a time reversal operator, the eigenvectors of which are linked to the targets. The

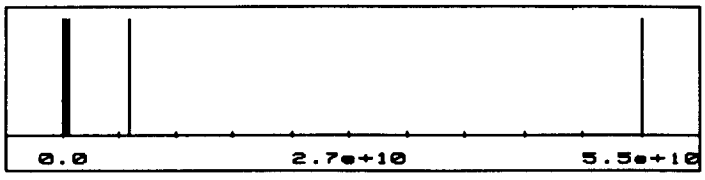


Fig. 14. Third experiment: Distribution of the 64 eigenvalues for the two spheres.

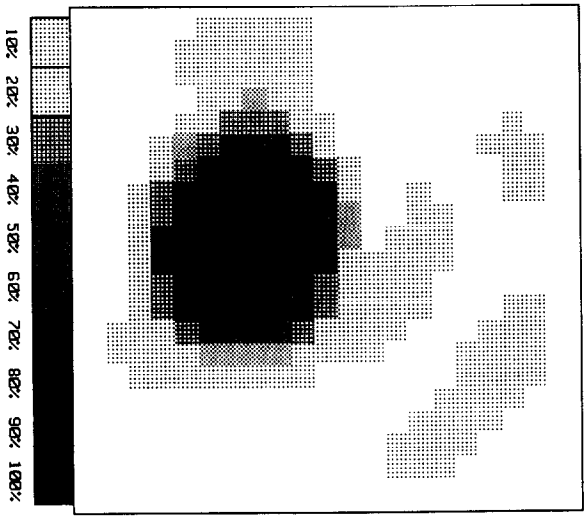


Fig. 15. Third experiment: Scanning of the field produced by propagation of the first eigenvector, scanned area 20×20 mm.

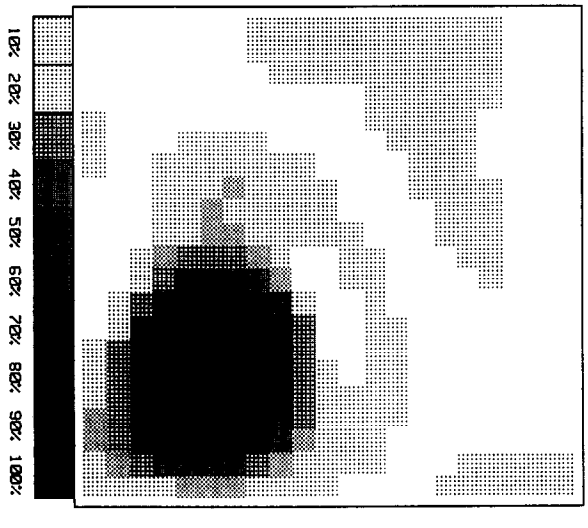


Fig. 16. Third experiment: Scanning of the field produced by propagation of the second eigenvector, scanned area 20×20 mm.

eigenvalue depends on the reflectivity of the target and the eigenvector provides the phase and amplitude law to focus on the target. The theoretical and experimental results show the efficiency of the method.

The applications of this method are numerous and are now studied in our laboratory in the field of lithotripsy and nondestructive testing.

## Appendix. Determination of the eigenvectors of the time reversal operator for the case of well resolved targets

If the input signal is the vector $\boldsymbol{H}_i^*$ with components $H_{i1}^*, H_{i2}^*, \ldots, H_{iL}^*$ then the received signal is $\mathbf{K}\boldsymbol{H}_i^*$. The component number $l$ of this vector is according to equation (17)

$$\sum_{m=1}^{L} K_{lm} H_{im}^* = \sum_{m=1}^{L} \sum_{k=1}^{d} H_{kl} C_k H_{km} H_{im}^* = \sum_{k=1}^{d} H_{kl} C_k \sum_{m=1}^{L} H_{km} H_{im}^* . \tag{A.1}$$

The sum over $m$ is the scalar product of vectors $\boldsymbol{H}_k$ and $\boldsymbol{H}_i$. The consequence of the ideal separation of the targets is that those two vectors are orthogonal for $k \neq i$ and Eq. (A.1) becomes

$$\sum_{m=1}^{L} K_{lm} H_{im}^* = H_{il} C_i \sum_{m=1}^{L} |H_{im}|^2 . \tag{A.2}$$

We see that the output vector $\mathbf{K}\boldsymbol{H}_i^*$ is proportional to $\boldsymbol{H}_i$. Eq. (A.2) can be put in a vector form

$$\mathbf{K}\boldsymbol{H}_i^* = C_i \sum_{m=1}^{L} |H_{im}|^2 \boldsymbol{H}_i . \tag{A.3}$$

This leads to the equation

$$\mathbf{K}^*\mathbf{K}\boldsymbol{H}_i^* = |C_i|^2 \left( \sum_{m=1}^{L} |H_{im}|^2 \right)^2 \boldsymbol{H}_i^* . \tag{A.4}$$

The eigenvalues are $|C_i|^2(\sum_{m=1}^{L}|H_{im}|^2)^2$ associated with the eigenvectors $\boldsymbol{H}_i^*$. We have proven that an eigenvector of the iterative time reversal operator is exactly the vector signal emitted after one time reversal for one target taken alone.

## References


[1] M. Fink, C. Prada, F. Wu and D. Cassereau, Self focusing with time reversal mirror in inhomogeneous media'' in *Proc. IEEE Ultrason, Symp.* 1989 2, 681–686 (1989).

[2] C. Prada, F. Wu and M. Fink, ''The iterative time reversal mirror: A solution to self-focusing in the pulse echo mode'' *J. Acoust. Soc. Am.* 90 (2), 1119–1129 (1991).

[3] M. Fink, ''Time reversal of ultrasonic fields – Part I: Basic principles'', *IEEE Trans. Ultrason., Ferroelec., Freq. Contr.* 39 (5), 555–1566 (1992).

[4] F. Wu, J.L. Thomas and M. Fink, ''Time reversal of ultrasonic fields – Part II: Experimental results'', *IEEE Trans. Ultrason., Ferroelec., Freq. Contr.* 39 (5), 567–578 (1992).

[5] D. Cassereau and M. Fink, ''Time-reversal of ultrasonic fields – Part III: Theory of the closed time-reversal cavity'', *IEEE Trans. Ultrason., Ferroelec., Freq. Contr.* 39 (5), 579–592 (1992).

[6] C. Prada, ''Retournement temporal des ondes ultrasonores: application à la focalisation'', *Thèse de doctorat de l'Université Paris VII* (June 1991).

[7] M. Fink, ''Time-reversal mirrors'', *J. Phys. D: Appl. Phys.* 26, 1333–1350 (1993).

[8] D.R. Jackson and D.R. Dowling, ''Phase conjugation in underwater acoustics'', *J. Acoust. Soc. Am.* 89, 171–181 (1991).

[9] D.R. Jackson and D.R. Dowling, ''Narrow-band performance of phase-conjugate arrays in dynamic random media'', *J. Acoust. Soc. Am.* 91 (6), 3257–3276 (1992).

[10] S.W. Flax and M. O'Donnel, ''Phase aberration correction using signals from point reflectors and diffuse scatterers: basic principle'', *IEEE Trans. Ultrason. Ferroelec., Freq. Control* 35, 758–767 (1988).

[11] L.D. Landau and E.M. Lifchitz, *Fluids Mechanics*, Pergamon, New York (1983).

[12] M Fink, J.F. Cardoso, ''Diffraction effects in pulse-echo measurement'', *IEEE Trans. on Sonics and Ultrasonics* 31 (4), 313–329 (1984).